Theoretical Analysis of a Fully Combustible Telescoped Round

M. S. NUSBAUM*
IIT Research Institute, Chicago, Ill.

A FULLY telescoped cartridge is one that completely contains the projectile, thereby requiring less ammunition storage than a conventional design and providing a geometry that is easier to feed. The use of combustible material reduces cost and weight, and eliminates the need for disposing of spent cases. A unique requirement of the interior ballistic design is that the projectile obturate the gun tube before an appreciable quantity of gas can blow-by. This Note describes a theoretical interior ballistic model formulated to represent the ballistic events and their sequence. Experimental evidence upon which to base the model was provided primarily by dynamic in-breech radiographs. Conventional interior ballistic calculations indicated that complete ignition took place after the projectile was in motion. In addition, firing data showed that under some conditions blow-by occurred. Thus, a model for the interior ballistics which would encompass the "delayed" ignition of the charges and permit blow-by was required.

The combustible material used for the 30-mm cartridge case (Fig. 1) is felted nitrocellulose reinforced with Kraft fiber and bonded with Formvar resin. The case structure is built up from two cylinders and four annular bulkheads. The igniter tube is a combustible case developed for a 7.62-mm round.[1] Typical experimental firing data are shown in Table 1. The analysis made was performed with IITRI's interior ballistics computer program, which is written in Fortran IV for an IBM 7094 computer. The code handles two different propellant formulations and a variety of grain geometries.

The Model and Its Calibration

The model provides an initial period of igniter action followed by full burning of the case material and propellant charge (main charges). Performance degradation was introduced through provision for gas and propellant to blow-by the projectile ogive until it fully obturates the bore. The

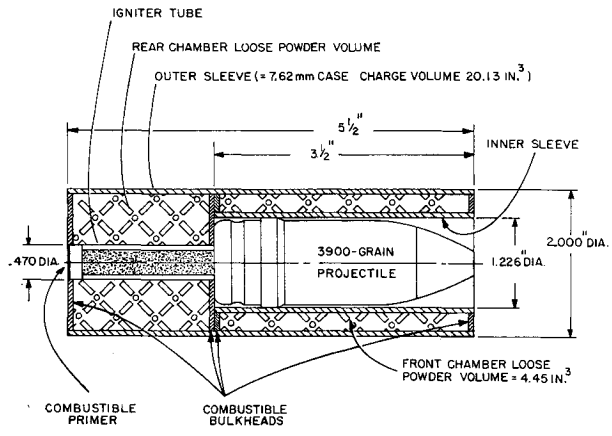

Fig. 1 Combustible-case 30 mm cartridge design; projectile travel to apturate barrel = 2.5 in., total weight of combustible material = 517.27 g, total volume of combustible material = 3.43 in.³

Presented as Paper 68-660 at the ICRPG/AIAA 3rd Solid Propulsion Conference, Atlantic City, N.J., June 4–6, 1968; submitted June 19, 1968; revision received October 8, 1968. Supported in part by Frankford Arsenal under Contract DAAA-25-67-C-0415.

* Manager, Ballistics and Explosives Section, Engineering Mechanics Division. Member AIAA.

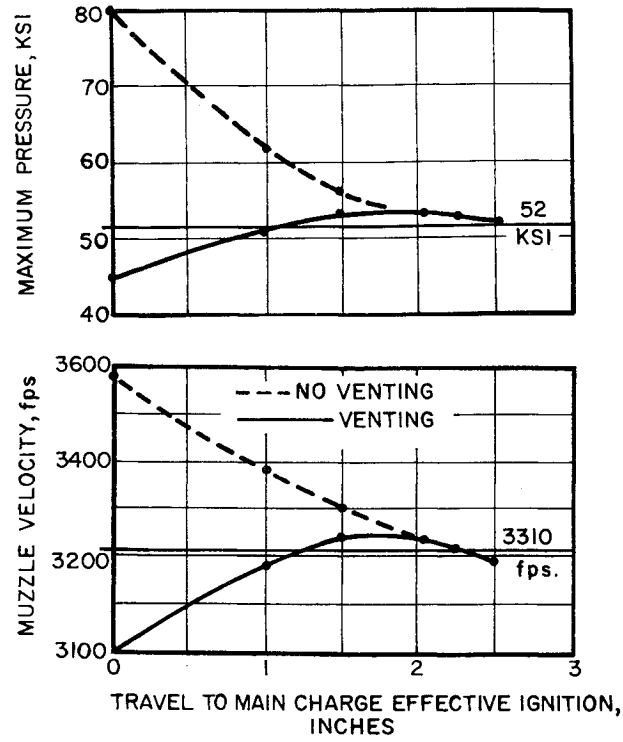

Fig. 2 Performance correlation curves, round 25.

parameters determined by repeated calculation and comparison to experimental data were bore friction profile, projectile travel to effective ignition of the charges, pressure and velocity at ignition of the charges, pressure at which blow-by starts, and the fraction of the gun charge lost during blow-by.

The computational procedure had four steps. First, igniter interior ballistic curves were obtained for each of the rounds under consideration. Output conditions of volume, pressure, and velocity corresponding to six projectile positions were used as input conditions for making the next series of calculations.

Using these basic input data, the bore friction profile was adjusted (the second step) until the maximum breech pressure P_{max} and muzzle velocity V_m calculated for rounds 25 and 36 fell on correlative curves, i.e., plots of V_m and P_{max} vs travel to effective ignition. The data point for round 24 was not on its correlation curve due to performance degradation.

The next step was the introduction of blow-by. The maximum pressure at which this degradation could be initiated without nullifying the performance match established for rounds 25 and 36† was selected as the criteria. This performance reduction was insufficient to provide good corre-

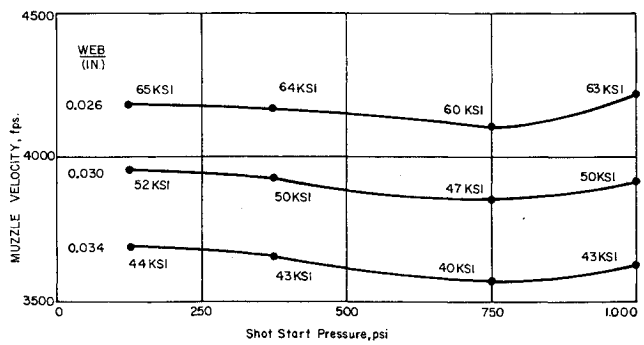

Fig. 3 Muzzle velocity vs shot-start pressure and IMR web.

† These rounds were assumed to provide data for undegraded cases. The introduction of gas blow-by slightly reduced the previously correlated performance for round 36.

Table 1 Data used to calibrate computer code[a]

Round	Propellant	Loading conditions: Behind projectile[b] Grains	Behind projectile η_ρ, %	Around projectile Grains	Around projectile η_ρ, %	V_m, fps	P_{max}, ksi
23	IMR4320	772	66.6	309	29.9	2810	36
24	IMR4320	1003	86.5	309	29.9	2990 (2996)	45 (44.7)
25	IMR4350	1154	99.0	386	37.1	3310 (3311)	52 (53)
26	IMR4350	1196	102.6	386	37.1	3070	56
36	IMR4350	1196	102.6	463	44.5	3500 (3480)	62 (61.4)

[a] Numbers in parentheses show outputs obtained
[b] η_ρ = percent of maximum theoretical density.

spondence between experimental and theoretical results for round 24. The final stage in calibration was the introduction of the propellant loss. Various loss fractions were tried until the final correlation was obtained.

Table 2 shows the bore resistance profile. The pressure at which blow-by started was established as 2500 psi. The calculated loss of solid gun charge, for round 24, was 2% of the main charge. The theoretical performances are shown parenthetically in Table 1. Table 3 shows the initial conditions, obtained from igniter calculations, which were used for round 25. Figure 2 shows P_m and V_m vs travel to assumed ignition of the main charges. The solid curves show the final calculations (with venting) and the broken line shows the calculations when no performance degradation was taken into account. The optimum design condition, in this case, is represented by the travel at which the two sets of curves become common.

Table 2 Bore resistance profile

	Before engraving	During engraving	After engraving
Travel	3.5 in.	1 cal	To muzzle
Resistance	50 psi	2500 psi	2200 psi

Parametric Investigation

A parametric investigation was conducted, using the calibrated model, to establish the potential performance that could be obtained from the 3900-grain, 30-mm round. The gun charge and combustible case weights were held fixed and it was assumed that Improved Military Rifle (IMR) propellant could be compacted and loaded at a density of 1.2 g/cm^3 without altering its burning characteristics. The "main-charge" variable was the IMR propellant web. The other parameters varied were those associated with igniter performance: velocity and pressure at the position of the projectile at effective ignition of the main charges. IMR 4198 (web = 0.01) was considered loaded in the igniter tube at a density 1.2 g/cm^3 for the first series of calculations. Igniter performance variations were obtained by assuming various values of the shot-start pressure P_{ss}. The maximum breech pressure and muzzle velocity resulting from igniter calculations which provided the shortest travel to effective main charge ignition without blow-by was selected as the data point to correlate web with the igniter, and P_{ss} was used as the igniter correlation parameter. The results are shown in Fig. 3. Both V_m and P_{max} increase as the IMR propellant web is reduced.

Table 3 Initial conditions used for calculating interior ballistics for round 25

Travel to ignition, in.	Space mean pressure, psi	Velocity, fps	Chamber volume, in.^{3}
0	338	0	13.00
0.98	358	55.4	14.14
1.50	326	71.7	14.75
2.05	311	82.0	15.39
2.26	309	84.8	15.65
2.53	299	89.6	15.96

The reasons for the reduction in P_{max} and V_m as P_{ss} is increased to 750 psi and the increases at 1000 psi can be discerned from the igniter input data. The initial conditions of travel, velocity, and pressure increase with P_{ss} until the pressure, at assumed ignition of the main charge, reaches the value represented by the P_{ss} = 750 psi condition. The combination of increased volume (by virtue of greater travel) more than offsets the higher pressure. But when $P_{ss} > 750$ psi, the effect of the higher igniter pressure is not offset, and P_{max} is increased due to earlier and more rapidly induced propellant burning. Further review of the calculations indicated that the time to effective ignition was lengthened by increasing P_{ss} because the burning rate of the combustible tube and igniter charge do not increase significantly over the range of P_{ss} used, hence the time to consume sufficient propellant to reach successively higher P_{ss} is increased. The increase in projectile velocity resulting from the higher starting pressure is insufficient to negate this effect. Table 4 shows the time to ignition T_i and total ballistic cycle time T_t correlated to P_{ss}. The study of the ignition design was continued by investigating the effect of its mass generation rate by considering slower propellant and other igniter loading densities $\rho_{l(1)}$. A slower propellant produces gas at a lower rate; similarly, reducing $\rho_{l(1)}$ will reduce the gas generation rate. Calculations were made considering IMR 3031 (web = 0.115 in. compared to IMR 4198, web = 0.01 in.) at the same $\rho_{l(1)}$, 1.2 g/cm^3, which increased T_t. The effects on P_{max} and V_m were minor (Table 4).

In terms of T_t, it can be seen that the web of the igniter charge is more significant than $\rho_{l(1)}$. The effects on V_m and P_{max} are relatively insignificant; however, there may be some latitude for minor optimization of the igniter charge in this regard.

Conclusion

The interior ballistic model will assist in the interpretation of experimental data and provide design guidelines for performance optimization. Further verification of the model should be undertaken by experimental measurement of the

Table 4 Ballistic results of shot-start and igniter parameter variations

P_{ss}, psi	$\rho_{l(1)}$, g/cm^3	IMR web, in.	T_i, msec	T_t, msec	P_{max}, ksi	V_m, fps
125	1.2	0.0100	6.33	8.49	65.0	4183
375	1.2	0.0100	6.72	8.92	64.0	4167
750	1.2	0.0100	7.19	9.24	60.0	4100
1000	1.2	0.0100	7.35	9.44	63.2	4209
1000	1.2	0.0115	8.95	11.00	62.1	4136
1000	1.0	0.0100	9.28	10.32	62.3	4178
1000	1.4	0.0100	6.77	8.82	63.1	4188

projectile position and velocity as well as the pressure that exists when the main charge components are fully ignited. There are limitations, as yet undefined, on the exploitation of the model (e.g., there are practical limits on the abilities of the combustible components to withstand the desired shot-start loads and to contain the pressure generated by the igniter). The capability for obtaining ignition at the desired projectile travel when ignition of the main charge components is desired must be determined through continued development. It appears that with some further development the felted nitrocellulose combustible case material will provide optimum cartridge interior ballistics.

Reference

[1] Zimmerman, F. J., "The Development of Small-Caliber Combustible-Cartridge-Case Ammunition," *Journal of Spacecraft and Rockets*, to be published.

Stress Analysis of Incompressible Solids of Revolution by Point Matching

F. R. Wallis*
Summerfield Research Station,†
Kidderminster, England

Nomenclature

A_n, B_n, B, k_i = coefficients determined by boundary conditions
a_{nk} = coefficients in polynomial solutions of biharmonic equation
$\mathbf{b}_1$, $\mathbf{b}_2$ = column vectors of right-hand sides of boundary equations
e = dilation
G = shear modulus
k, n, s = nonnegative integers
M_1, M_2 = coefficient matrices in boundary equations
m = number of terms in a polynomial summand
N = upper summation limit for n
r, z = radial and axial cylindrical coordinates
u, w = radial and axial displacements
$\mathbf{x}$ = column vector of solutions to boundary equations
X, Z = radial and axial components of body force
β = limit of $e/(2\nu - 1)$ as $\nu \to \frac{1}{2}$
$\mathfrak{X}$ = column vector of dummy unknowns
ν = Poisson's ratio

Introduction

SOLID-propellant rocket charges undergo stresses and strains under conditions imposed by differential contraction of propellant and case after curing and in storage, axial acceleration and spin in flight, or pressurization during firing. Each of these factors, or a combination of them, may cause mechanical failure in the propellant itself, or at a bond with the case. Another category of failure is deformation of the conduit, which, although not a mechanical failure, may have a significant effect on the internal ballistics. Before failure criteria can be applied, a detailed knowledge of the stresses and strains is required. In principle the method herein could be applied to the biharmonic equation in a single axisymmetric stress function,[1] but the following incompressible analysis is simpler and has wide application to charges of virtually incompressible propellant. Approximate solutions for finite cylinders by station functions[2,3] have been obtained in closed form. The point matching solutions are also in closed form and satisfy the equilibrium equations exactly, but approximate to the boundary conditions by regression on selected boundary points. Recently, Hooke[4] applied the technique to plane situations exhibiting local stress concentrations, using a least-squares fit to the values at the boundary points.

The analysis below applies to any solid of revolution composed of an incompressible homogeneous isotropic elastic material under conditions of small strain. The axial component of the body force must be constant radially, and the radial component must be constant axially. Any axisymmetric boundary conditions that are consistent with incompressibility may be applied, provided that at least one value of a direct stress is given. The boundary points are fitted by least squares, with an optional subset matched exactly. An exact fit to all points will generally result in excessive inter-point deviations.

Analysis

The condition of incompressibility and the equilibrium equations give

$$\partial u/\partial r + u/r + \partial w/\partial z = 0 \tag{1}$$

$$\partial \beta/\partial r = \partial^2 u/\partial z^2 - \partial^2 w/\partial r \partial z + X/G \tag{2}$$

$$\partial \beta/\partial z = \nabla^2 w + Z/G \tag{3}$$

Subject to the conditions that $\partial X/\partial z = \partial Z/\partial r = 0$, u and β are eliminated from Eqs. (1–3) to yield

$$\nabla^4 w = 0 \tag{4}$$

Equation (4) has a standard solution[1] consisting of two independent series of homogeneous polynomials. These series are truncated to give

$$w = \sum_{n=1}^{N} A_n \sum_{k=1}^{m} a_{nk} z^{n-2(k-1)} (z^2 + r^2)^{k-1} + \sum_{n=0}^{N} B_n \sum_{k=1}^{m} a_{nk} z^{n-2(k-1)} (z^2 + r^2)^k \tag{5}$$

where $a_{n1} = 1$ and

$$a_{nk} = -\tfrac{1}{2} a_{n,(k-1)} (n - 2k + 4) \times (n - 2k + 3)/(k - 1)(2n - 2k + 3)$$

for $k = 2$ to m, and m is the integral part of $\frac{1}{2}(n + 2\frac{1}{2})$. The coefficients A_n, B_n are arbitrary. Using the notation (k,s) for binomial coefficients, Eq. (5) may be written

$$w = \sum_{n=1}^{N} A_n \sum_{k=1}^{m} a_{nk} \sum_{s=0}^{k-1} (k-1,s) z^{n-2s} r^{2s} + \sum_{n=0}^{N} B_n \sum_{k=1}^{m} a_{nk} \sum_{s=0}^{k} (k,s) z^{n-2s+2} r^{2s} \tag{6}$$

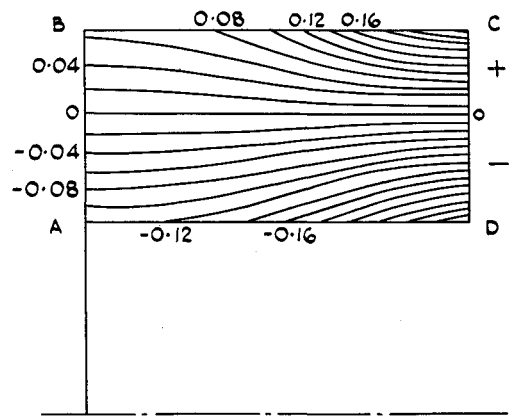

Fig. 1 Level lines of axial stress/shear modulus.

Received June 14, 1968.

* Technical Officer, Rocket Motor Design and Development Department.

† Operated on behalf of the Ministry of Technology by Imperial Metal Industries Ltd., a subsidiary company of Imperial Chemical Industries Ltd.